Off-site control of repolarization alternans in canine cardiac Purkinje fibers

Trine Krogh-Madsen[1], David J. Christini[1,2], Peter J. Jordan[2],
Mark L. Riccio[3], Robert F. Gilmour, Jr.[3], and Alain Karma[4]
[1]*Division of Cardiology, Department of Medicine,*
Weill Cornell Medical College, New York, New York 10021,
[2]*Department of Physiology and Biophysics,*
Weill Cornell Medical College, New York, New York 10021

(Dated: February 20, 2009)

Abstract

Repolarization alternans, a beat-to-beat alternation in action potential duration, has been causally linked to the onset of cardiac reentry. Anti-alternans control strategies can eliminate alternans in individual cells by exploiting the rate dependence of action potential duration. The same approach, when applied to a common measuring/stimulating site at the end of a cardiac fiber, has been shown to have limited spatial efficacy. As a first step towards spatially distributed electrode control systems, we investigated "off-site" control in canine Purkinje fibers, in which the recording and control sites are different. We found that alternans can be eliminated at, or very near, the recording site, and that varying the location of the recording site along the fiber causes the node (the location with no alternans) to move along the fiber in close proximity to the recording site. Theoretical predictions based on an amplitude equation agree with our experimental findings, and illustrate how the deviation between the recording site and the actual position of the node is dependent upon electrotonic effects. Computer simulations using a Purkinje fiber model confirm these theoretical and experimental results. Although off-site alternans control does not suppress alternans along the entire fiber, our results indicate that placing the node away from the stimulus site reduces alternans amplitude along the fiber, and may therefore have implications for anti-arrhythmic strategies based on alternans termination.

PACS numbers:

I. INTRODUCTION

When paced rapidly, cardiac cells often exhibit a type of dynamics called repolarization alternans, which is a beat-to-beat alternation in the duration of the action potential. In the heart, such alternans induces spatial and temporal dispersion in refractoriness, which increases the risk of occurrence of potentially fatal cardiac arrhythmias. This is particularly the case when the tissue exhibits spatially discordant alternans, where different regions are alternating out of phase. Evidence of causality between alternans and the onset of arrhythmias has been demonstrated in both experiments [1, 7, 11] and computer simulations [7, 12].

Because of this link, alternans control targeted at eliminating alternans is currently under investigation as a potential antiarrhythmic strategy. Most of this work is based on model-independent, adaptive control algorithms, e.g., delayed feedback control (DFC). In this method, which is based on the Ott-Grebogi-Yorke (OGY) [10] technique for chaos control, small perturbations are applied to the timing of the next excitation in an attempt to force the state of the system toward the (unstable) period-1 fixed point.

DFC has been used experimentally to control repolarization alternans in small pieces (i.e., sufficiently small to be point-like) of bullfrog hearts [8]. DFC algorithms have also been used to control a related type of alternans (atrioventricular (AV) nodal conduction alternans; a beat-to-beat alternation in the conduction time through the AV node) [2, 4, 9]. To date, AV node alternans control is the only alternans control study performed on human subjects.

While repolarization alternans may be successfully eliminated in a system that does not have spatiotemporally varying repolarization and wave-propagation dynamics, initial analytical work as well as computer simulations of one-dimensional tissue fibers suggest that only in the case of spatially uniform alternans of small amplitude can alternans be terminated along the whole fiber. In cases where concordant alternans show variation in space, as well as in the more extreme cases of spatially discordant alternans, eliminating alternans at one site will result in alternans being eliminated only up to a short distance away from this stimulation site [3, 5]. Experiments in canine Purkinje fibers qualitatively confirm these predictions [3].

These studies therefore suggest that spatially distributed multiple-electrode systems will be necessary in order to eliminate repolarization alternans in the heart. As a first step

towards this goal, we decided to investigate the possibility of recording action potential duration data from one location and use that at a remote stimulus site. In experiments on canine Purkinje fibers as well as in computer simulations we show here that by applying this type of off-site control, alternans can be eliminated at a desired location which can be far away from the stimulus site.

II. METHODS

A. Ex vivo recordings

B. Coupled map model

Because of limitations of existing ionic Purkinje fiber models in reproducing basic experimental findings such as the conduction velocity (CV), we have utilized a coupled maps model such as that of Ref.[6]. This model is based on fits to experimental action potential duration (APD) and CV restitution curves. The model equations are:

$$\mathrm{APD}_{i+1} = f(\mathrm{DI}_i) + \xi^2 \nabla^2 \mathrm{APD}_{i+1} - w \nabla \mathrm{APD}_{i+1} \tag{1}$$

$$\mathrm{DI}_{i+1}(x_i) = T + \sum_{j=0}^{i-1} \frac{\Delta x}{\theta(\mathrm{DI}_{i+1}(x_j))} - \sum_{j=0}^{i-1} \frac{\Delta x}{\theta(\mathrm{DI}_i(x_j))} - \mathrm{APD}_{i+1}(x_i), \tag{2}$$

where $f(\mathrm{DI}_i) = 31 + 160/(1+\exp(-(\mathrm{DI}_i - 43)/36))$ is the APD restitution curve, $\theta(\mathrm{DI}_i) = 1 + 1.4/(1+\exp(-(\mathrm{DI}_i - 7)/1.4))$ is the CV restitution curve, and T is the pacing cycle length. The parameter ξ determines spatial coupling. We set $\xi = 0.1$ cm so that discordant alternans occurred at a pacing rate similar to that seen in our experiments, and $w = 0.002$ cm. No-flux boundary conditions were implemented. When Eqn. 1 is discretized using forward finite differences with a three-point stencil for the Laplacian, the solution is obtained by solving a linear tri-diagonal matrix system. We used a fiber length of $L = 2$ cm, which is similar to the length of the canine Purkinje fiber, and a Δx of 0.01 cm.

C. Alternans control

As in our previous work [3], we apply a delayed feedback control algorithm, but we now separate the stimulus site and the recording site

$$T_{n+1}(0) = \begin{cases} T^\star & \text{for} \quad \Delta T_{n+1} > 0, \\ T^\star + \Delta T_{n+1} & \text{for} \quad \Delta T_{n+1} \leq 0, \end{cases} \tag{3}$$

with

$$\Delta T_{n+1}(0) = \frac{\gamma}{2} \left[\mathrm{APD}_{n+1}(x_r) - \mathrm{APD}_n(x_r) \right], \tag{4}$$

where γ is the feedback gain and $\mathrm{BCL}^\star$ is the nominal BCL. We use $x = 0.0$ cm as the stimulus site, but vary the recording site (x_r), at which successive APD values are measured, along the fiber. We use $\gamma/2 = 0.5$, except when otherwise noted (Fig. 6). *also true for exps?*

III. RESULTS

A. Experimental results

In a previous study, we have shown that when applying alternans control from a common recording/stimulating site at the proximal end of a Purkinje fiber alternans may be diminished at that location, but persists distal to it [3]. An example of this type of control dynamics is shown in Fig. 1(b). Based on this result, we hypothesized that using APD values recorded at more distal locations on the fiber, while keeping the stimulus site at the proximal end, would cause an APD node to be formed at the recording location, i.e., that alternans would be eliminated at the recording site, but not away from it. Using six recording electrodes placed equidistantly along the 2 cm fiber, we found that this is indeed the case [Fig. 1(c-g)]. Hence, by applying this type of off-site control, APD alternans can be eliminated at any desired location which can be far away from the stimulus site.

B. Simulation results

In order to investigate the non-local control in more detail, we used a coupled map model based on experimentally recorded APD and CV restitution curves (see Methods). When applying on-site control, APD alternans is almost entirely eliminated at the proximal end,

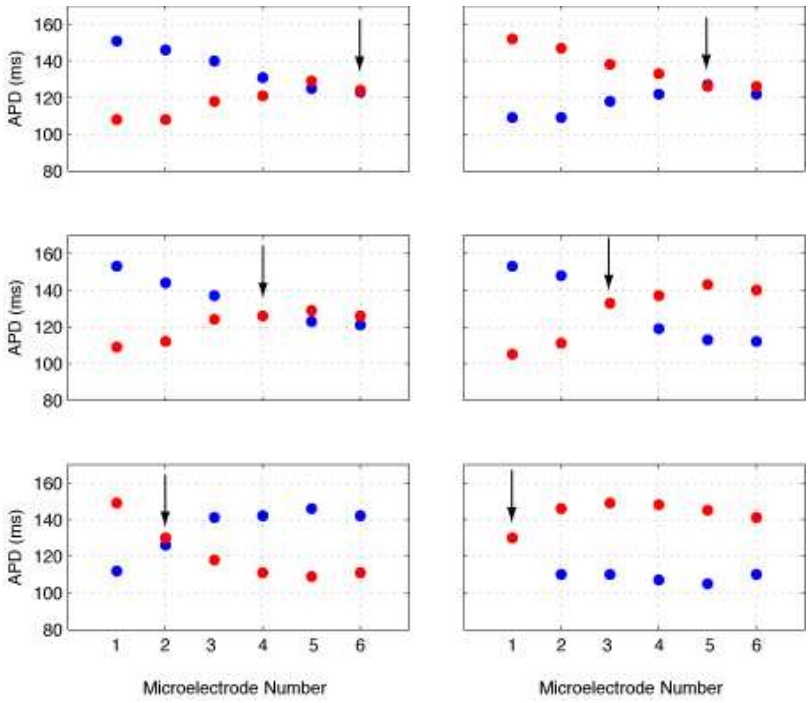

Figure X. Non-local control of APD dynamics in a canine cardiac Purkinje fiber. APD of *n* (red) and *n+1* (blue) beats are displayed at equally spaced recording sites (1-6) along the fiber. The recording site used for control (arrow) was shifted sequentially from site 6 (upper left panel) to site 1 (lower right panel). Note adequate control of APD alternans at the control site, with deviation of APD spatially about the control site.

FIG. 1: Should be (a) no control, (b)-(g) control at microelectrode 1-6. Representative example. Such node placement occurred robustly in x experiments in y different fibers.

but persists distally, in agreement with our previous experimental and theoretical results [Fig. 2(b)] [3]. When applying off-site control using the locations corresponding to the remaining five microelectrodes in the experiments, the same phenomenon occurs: APD alternans is diminished at the recording site, but persists away from it [Fig. 2(c-g)].

When x_r is not located at either end of the cable, the diminishing of APD alternans manifests as an APD node (where APD is constant) separating out-of-phase regions [Fig. 2(c-f)]. This node forms very close to x_r. In the cases where x_r is located at either the proximal or the distal end, no node is formed, but the APD alternans magnitude displays a minimum at x_r [Fig. 2(b and g)].

The APD profiles are very near symmetric with respect to the recording site, such that the profiles for $x_r = 2.0$ cm (1.6, 1.2) are mirror images of those for $x_r = 0.0$ cm (0.4, 0.8). Such symmetry is found for a range of relatively slow pacing rates (yet fast enough

to induce alternans). However, for faster pacing rates, the spatial symmetry starts to break and the APD profiles become slightly asymmetric, similar to the asymmetry observed in the experimental recordings (Fig. 1). Such asymmetry is consistent with the effects of CV restitution at fast pacing [12, 13], and, indeed, in our coupled maps simulations, it disappears when the CV restitution function is replaced by a constant value.

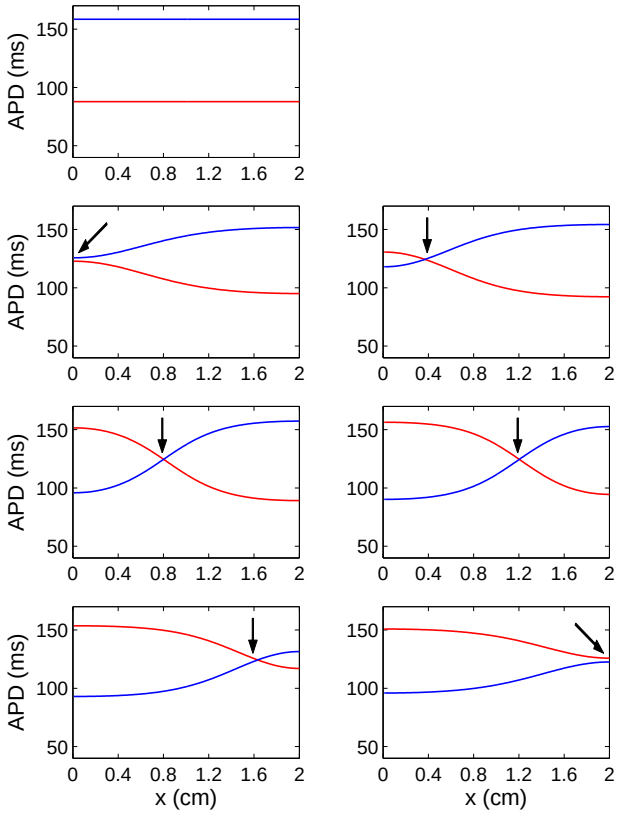

FIG. 2: Non-local control in coupled maps model with a BCL of 180 ms. (a) No control, (b)-(g) control at locations $x_r = 0.0$, 0.4 0.8, 1.2, 1.6, and 2.0 cm (indicated by arrows).

At even faster pacing, a discordant node forms prior to the application of alternans control [Fig. 3(a)]. In this case, off-site control is still successful in eliminating alternans close to the recording site, but the position of the resultant node is further from x_r when x_r is towards the distal end of the fiber.

Figure 4 shows a summary of the pacing rate dependence using the spatially averaged alternans magnitude as a measure of the effect of the off-site control application. The alternans magnitude is greatly reduced when the recording site is towards the middle of the cable. More proximal or distal recording sites also reduce the alternans magnitude

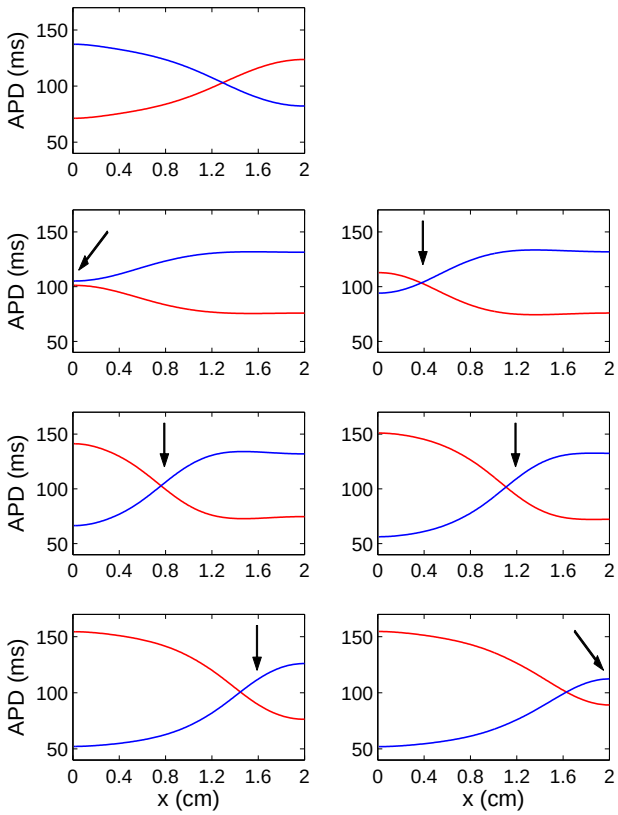

FIG. 3: Non-local control of spatially discordant alternans in coupled maps model with a BCL of 140 ms. (a) No control, (b)-(g) control at locations $x_r = 0.0$, 0.4 0.8, 1.2, 1.6, and 2.0 cm (indicated by arrows).

significantly, except when there is spatially discordant alternans prior to control (BCL = 140 ms). Only in the case of spatially uniform and relatively small-amplitude concordant alternans (BCL = 200 ms), is alternans eliminated throughout the fiber, both for on-site and off-site control.

C. and we have a theory, too!

The APD at the n^{th} beat along the cable for the fundamental standing wave mode neglecting CV restitution effects is given by:

$$\mathrm{APD}^n = \mathrm{APD}_c + (-1)^n a(x) \tag{5}$$

where APD_c is the APD at the periodic fixed point of the map and

$$a(x) \approx a(L)/2 \cos\frac{\pi x_r}{L} + \left(\frac{\pi^2\xi^2}{\gamma L^2} - 1\right)\cos\frac{\pi x}{L}, \tag{6}$$

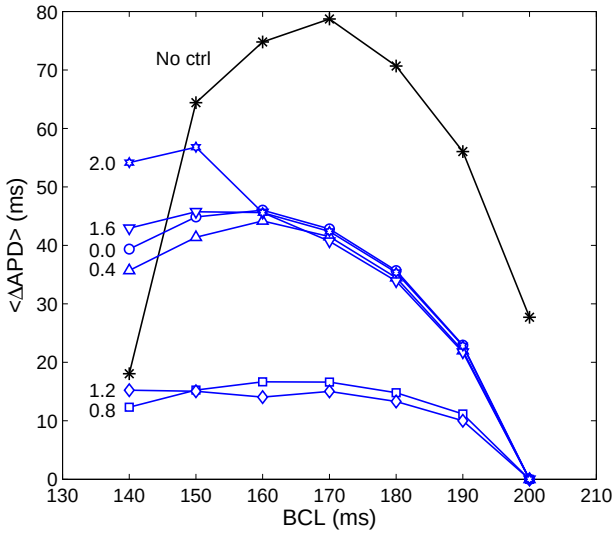

FIG. 4: Effects of off-site control on alternans amplitude. Numbers indicate values of x_r. Prior to control, there is spatially concordant alternans for pacing rates 150-190 ms and spatially discordant alternans at a pacing rate of 140 ms.

where ξ is the spatial coupling length and L is the fiber length. Figure 5 shows the resulting alternans amplitude spatial profiles for the same values of x_r as used in Figs. 1-4. These profiles are very similar to those obtained from the simulations *(and exp?)* in terms of the gradient and the node placement.

The position x_0 of the node (where the APD is constant from beat to beat) is found by setting $a(x_0) = 0$, which gives,

$$x_0 = \frac{L}{\pi} \cos^{-1} \left[\frac{1}{1 - (\pi^2 \xi^2)/(\gamma L^2)} \cos \frac{\pi x_r}{L} \right]. \tag{7}$$

The curve x_0 versus x_r therefore has a point symmetry about the center of the cable. For $\xi = 0$ (negligible diffusive coupling), this curve is just a straight line, meaning that the node and the recording site coincide. For finite coupling, however, a node only forms when $x_r^{min} \leq x_r \leq x_r^{max}$ where

$$x_r^{min} = \frac{L}{\pi} \cos^{-1} \left[1 - \frac{\pi^2 \xi^2}{\gamma L^2} \right] \tag{8}$$

and by symmetry

$$x_r^{max} = L - x_r^{min}. \tag{9}$$

The node position varies continuously from 0 to L as x_r varies from x_r^{min} to x_r^{max}. For x_r smaller than x_r^{min} or larger than x_r^{max}, there is no node; the amplitude of alternans is reduced

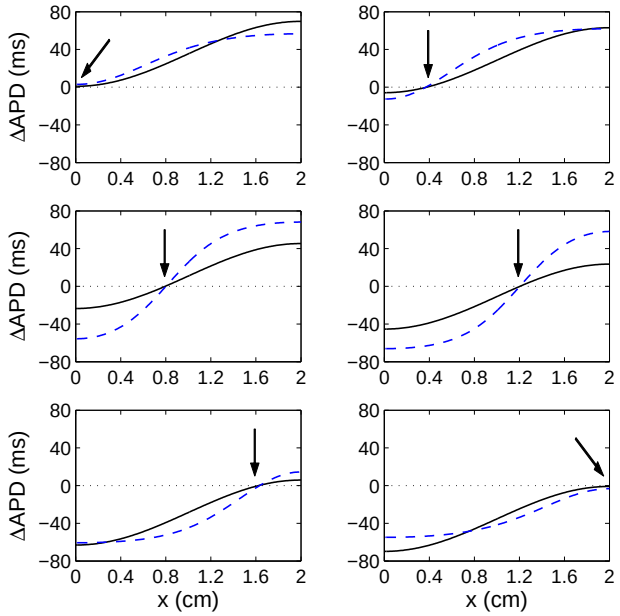

FIG. 5: Alternans amplitude (ΔAPD) profiles with off-site control applied at at locations $x_r = 0.0$, 0.4 0.8, 1.2, 1.6, and 2.0 cm (indicated by arrows). Theoretical profiles (solid, black lines) are computed from Eqn. x with $a(L)/2 = 70.7$ ms and compared to profiles from the coupled maps simulations (dashed, blue lines) with BCL = 180 cm (as in Fig. x). ******Add some exp data if available****

by control but does not vanish — exactly what we see in our simulations. Further, this result show that the deviation between the recording site and the node position is dependant upon electrotonic effects.

Figure 6(a) shows plots of the node position for different values of the feedback gain parameter γ. Interestingly, decreasing the feedback gain increases $1/[1-(\pi^2\xi^2)/(\gamma L^2)]$, and hence increases the departure from a straight line. The same phenomenon is observed in our simulations [Fig. 6(b)].

IV. DISCUSSION

Previous studies have suggested that elimination of repolarization alternans in spatially distributed systems using a common measuring/stimulus site is not possible over very large distances [3, 5]. Here, we use different measuring and stimulus sites to show that alternans may be controlled at specific desired locations which can be far away from the stimulus site.

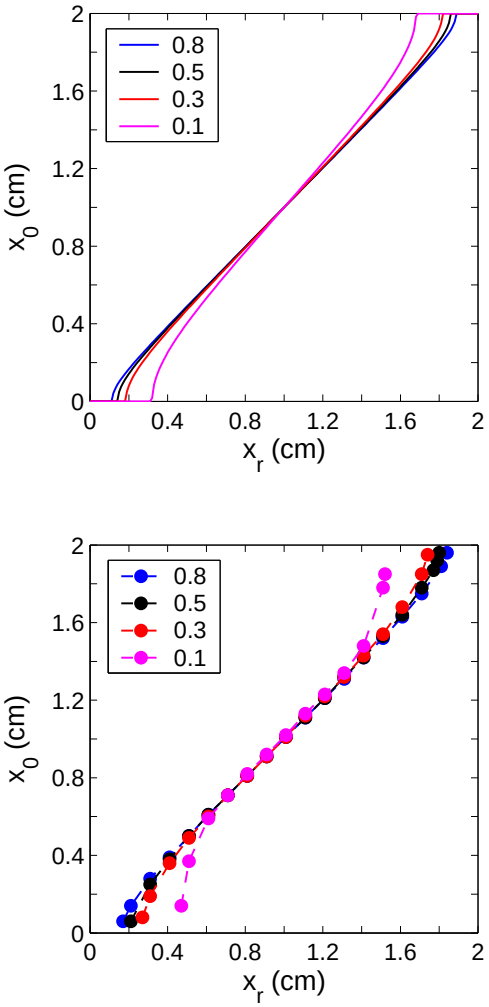

FIG. 6: Dependence of node position for off-site control on the feedback gain, $\gamma/2$. Analytical results (Eqn. x; solid lines) and simulation results (symbols and dashed lines) obtained for $\gamma/2 =$ 0.8 (blue), 0.5 (black), 0.3 (red), and 0.1 (magenta).

Such node placement not only robustly manifests over a large range of values of the feedback gain, but actually depends predictively on the gain.

The spatial alternans magnitude profile is well described by a theoretically described amplitude equation, which also predicts quantitatively the node placement. These findings thus further confirms the wave nature of alternans.

Although off-site control does not typically eliminate alternans everywhere along the fiber, it may still be potentially important for antiarrhythmic strategies. First, because it is a step towards multiple-electrode control. And second, because APD alternans amplitude varies spatially across the ventricles (with typically larger amplitude at the base than at the

apex). Hence, control may be most antiarrhythmic by modifying the pacing period from the measurement of APD where its amplitude is largest in the absence of control.

V. APPENDIX

Derivation of amplitude eqn.

---

[1] Masaomi Chinushi, Dmitry Kozhevnikov, Edward B. Caref, Mark Restivo, and Nabil El-Sherif. Mechanism of discordant T wave alternans in the in vivo heart. *Journal of Cardiovascular Electrophysiology*, 14:632–638, 2003.

[2] David J. Christini and James J. Collins. Using chaos control and tracking to suppress a pathological nonchaotic rhythm in a cardiac model. *Physical Review E*, 53:R49–R52, 1996.

[3] David J. Christini, Mark L. Riccio, Calin A. Culianu, Jeffrey J. Fox, Alain Karma, and Robert F. Gilmour, Jr. Control of electrical alternans in canine cardiac Purkinje fibers. *Physical Review Letters*, 96:104101–1 – 104101–4, 2006.

[4] David J. Christini, Kenneth M. Stein, Steven M. Markowitz, Suneet Mittal, David J. Slotwiner, Marc A. Scheiner, Sei Iwai, and Bruce B. Lerman. Nonlinear-dynamical arrhythmia control in humans. *Proceedings of the National Academy of Science*, 98:5827–5832, 2001.

[5] Blas Echebarria and Alain Karma. Spatiotemporal control of cardiac alternans. *Chaos*, 12(3):923–930, 2002.

[6] Jeffrey J. Fox, Mark L. Riccio, Paul Drury, Amanda Werthman, and Robert F. Gilmour, Jr. Dynamic mechanism for conduction block in heart tissue. *New Journal of Physics*, 5:101.1–101.14, 2003.

[7] Jeffrey J. Fox, Mark L. Riccio, Fei Hua, Eberhard Bodenschatz, and Robert F. Gilmour, Jr. Spatiotemporal transition to conduction block in canine ventricle. *Circulation Research*, 90:289–296, 2002.

[8] G. Martin Hall and Daniel J. Gauthier. Experimental control of cardiac muscle alternans. *Physical Review Letters*, 88:198102, 2002.

[9] Kevin Hall, David J. Christini, Maurice Tremblay, James J. Collins, Leon Glass, and Jacques Billette. Dynamic control of cardiac alternans. *Physical Review Letters*, 78:4518–4521, 1997.

[10] Edward Ott, Celso Grebogi, and James A. Yorke. Controlling chaos. *Physical Review Letters*, 64:1196–1199, 1990.

[11] Joseph M. Pastore, Steven D. Girouard, Kenneth R. Laurita, Fadi G. Akar, and David S. Rosenbaum. Mechanism linking T-wave alternans to the genesis of cardiac fibrillation. *Circulation*, 99:1385–1394, 1999.

[12] Zhilin Qu, Alan Garfinkel, Peng-Sheng Chen, and James N. Weiss. Mechanisms of discordant alternans and induction of reentry in simulated cardiac tissue. *Circulation*, 102:1664–1670, 2000.

[13] Mari A. Watanabe, Flavio H. Fenton, Steven J. Evans, Harold M. Hastings, and Alain Karma. Mechanisms for discordant alternans. *Journal of Cardiovascular Electrophysiology*, 12:196–206, 2001.